Sb-rich titanite in the manganese concentrations at St. Marcel-Praborna, Aosta Valley, Italy: petrography and crystal-chemistry

ELENA-ADRIANA PERSEIL [1,2] AND DAVID C. SMITH [1]

[1] Muséum National d'Histoire Naturelle, Laboratoire de Minéralogie, [2] CNRS, Unité de Recherche Associée n° 736, 61 Rue Buffon, 75005 Paris, France

Abstract

Titanites rich in antimony (up to 12.59 wt.% Sb_2O_5; equal to 0.165 Sb^{5+} per Si^{4+} = 1.000) are described for the first time. They coexist with various greenschist-facies minerals in three different petrographical environments in the manganese concentrations at St. Marcel-Praborna in the Aosta Valley, Italy. These titanites are chemically zoned, the Sb-richest parts generally occurring alongside grain boundaries, microfractures, pores or inclusions. Moderately-good positive correlations exist between the Sb, Al and Fe contents, with negative correlations of each of these elements with Ti. Cr has perturbed the Al and Fe contents since a better negative correlation with Ti is obtained with [Al + Cr + Mn + Fe]. The Sr, Ba, Mn and F contents are rather small and vary irregularly. Several crystal-chemical hypotheses are presented concerning the method of structural formula calculation and the valencies and site distributions of Sb and the companion additional minor elements. The favoured interpretation is to place: Sr^{2+}, Ba^{2+}, Mn^{2+}, Fe^{2+} and possibly also Sb^{3+} in the $^{vii}Ca^{2+}$ site; Sb^{5+}, Cr^{3+}, Al^{3+}, Sb^{3+}, Fe^{3+} and possibly also Mn^{3+} in the $^{vi}Ti^{4+}$ site; and Al^{3+} in the $^{iv}Si^{4+}$ site; this indicates the existence of a natural silicate containing not only both trivalent and pentavalent Sb, but also both valencies in the same site. The principal ionic substitution is believed to be: 2 $^{vi}Ti^{4+}$ = $^{vi}[Al^{3+} + Cr^{3+} + Mn^{3+} + Fe^{3+}] + {}^{vi}Sb^{5+}$ accompanied by a substantial minor proportion of: 2 $^{vi}Ti^{4+}$ = $^{vi}Sb^{3+} + {}^{vi}Sb^{5+}$, or possibly = 2 $^{vi}Sb^{4+}$ The data indicate a very late stage penetration of pre-existing titanites by mobilized Sb, Al, Cr, Mn, Fe, F and presumably also (OH) at this locality, whereas Sr and Ba were mobile at an earlier stage. Manganese, which existed in the sedimentary protoliths, did not enter the titanite structure in very significant quantities.

KEYWORDS: antimony, titanite, crystal-chemistry, petrography, St. Marcel-Praborna, Italy.

Introduction

THE manganese concentrations of St. Marcel-Praborna are restricted to a 4 to 8 m thick quartzite unit of diverse lithologies, textures and colours, which represents the heterogeneous basal part of the sedimentary cover of an ophiolite suite. Together they constitute a part of the Piemont Nappe which was metamorphosed up to the eclogite facies (jadeite present) in Cretaceous times and was retrogressed in the early Tertiary. The quartzite unit is composed of a succession of siliceous levels characterized by manganese-bearing mineral associations reflecting differences in chemical composition and f_{O_2} inherited from the original sediments. The parageneses evolved during the polyphasic Alpine metamorphism passing through a pre-eclogite blueschist-facies event, the main eclogite-facies event, and then several post-eclogite stages terminating in the greenschist facies (e.g. Martin-Vernizzi, 1982; Mottana, 1986; Martin and Kienast, 1987).

Many minerals in the manganese concentrations display Mn-bearing species or varieties (principally pink, purple, violet or black in colour) which may be rich or poor in Mn, for example: 'alurgite' (muscovite or phengite); birnessite; braunite; cryptomelane; hausmannite; hollandite; manganite; piemontite; priderite; pyrolusite; pyroxmangite; rhodochrosite; rhodonite; roméite; spessartine; rutile; 'violan' (diopside–aegirine–jadeite); (e.g. de Lom, 1843; Dufrenoy, 1847; Mottana *et al.*, 1979; Kienast *et al.*, 1982; Mottana, 1986; Martin and

Mineralogical Magazine, December 1995, Vol. 59, pp. 717–734

TABLE 1. Assignment of chemical elements to the different sites in titanite $XYO^{O1}ZO_4$, with ionic charges and radii, listed in order of increasing ionic radius (round brackets), appropriate to the co-ordinations (square brackets)

X or Ca site [vii], valencies 1^+, $\mathbf{2^+}$, 3^+ or 4^+:

Cr^{3+}	(>0.62)	Mn^{3+}	(>.64)	Fe^{3+}	(0.71)	Sb^{3+}	(>0.76)
Mg^{2+}	(0.80)	*Cr^{2+}*	*(>0.80)*	Sc^{3+}	(~0.81)	Fe^{2+}	(0.85)
Pb^{4+}	(~0.86)	Li^+	(0.88)	Mn^{2+}	(0.90)	U^{4+}	(0.95)
Y^{3+}	(0.96)	Th^{4+}	(1.00)	U^{3+}	(>1.03)	**Ca^{2+}**	**(1.06)**
Ce^{3+}*	(1.07)	Bi^{3+}	(~1.1)	Na^+	(1.12)	Sr^{2+}	(1.21)
Pb^{2+}	(1.23)	Ba^{2+}	(1.38)	K^+	(1.46)		

range: >0.62–1.46 * = one example of REE^{3+}

Y or Ti site [vi], valencies 2^+, 3^+, $\mathbf{4^+}$ or 5^+:

Cr^{5+}	(>0.49)	Mn^{4+}	(0.53)	Al^{3+}	(0.54)	Cu^{3+}	(0.54)
V^{5+}	(0.54)	Cr^{4+}	(0.55)	V^{4+}	(0.58)	Sb^{5+}	(0.60)
Ti^{4+}	**(0.60)**	Mo^{5+}	(0.61)	Cr^{3+}	(0.62)	V^{3+}	(0.64)
Nb^{5+}	(0.64)	Ta^{5+}	(0.64)	Fe^{3+}	(0.64)	Mn^{3+}	(0.64)
Mo^{4+}	(0.65)	*Ti^{3+}*	*(0.67)*	Nb^{4+}	(0.68)	Ta^{4+}	(0.68)
Mo^{3+}	(0.69)	Sn^{4+}	(0.69)	Mg^{2+}	(0.72)	Nb^{3+}	(0.72)
Ta^{3+}	(0.72)	Zr^{4+}	(0.72)	Cu^{2+}	(0.73)	Sc^{3+}	(0.74)
U^{5+}	(0.76)	Sb^{3+}	(0.76)	Bi^{5+}	(0.76)	Fe^{2+}	(0.78)
Pb^{4+}	(0.78)	V^{2+}	(0.79)	*Cr^{2+}*	*(0.80)*	Mn^{2+}	(0.83)
U^{4+}	(0.89)	Th^{4+}	(0.94)				

range: >0.49–0.94

Z or Si site [iv], valencies 3^+, $\mathbf{4^+}$ or 5^+:

P^{5+}	(0.17)	**Si^{4+}**	**(0.26)**	V^{5+}	(0.36)	Al^{3+}	(0.39)
Mn^{4+}	(0.39)	Cr^{4+}	(0.41)	Ti^{4+}	(0.42)	Mo^{5+}	(0.46)
Fe^{3+}	*(0.49)*	*Mn^{3+}*	*(<0.58)*	*Cr^{3+}*	*(<0.62)*	$4H^+$	(????)

range: 0.17–*<0.62*

O1 site [vi], valencies 1^- or $\mathbf{2^-}$:

F^-	(1.33)	OH^-	(1.37)	**O^{2-}**	**(1.40)**	Cl^-	(1.61)

range: 1.33–1.61

Notes:
— Chemical elements from the lists in the reviews published by Sahama (1946), Ribbe (1980), Deer *et al.* (1982) and Oberti *et al.* (1991), with Sb^{3+} and Sb^{5+} added here, as well as several valencies which are unusual for geologists but not for chemists.
— Ionic radii from Shannon (1976), the values for **pure $CaTiOSiO_4$ titanite being printed in bold type.**
— Ranges of ionic radii for the listed ions in each site, but not all of them have been proved to exist in natural or synthetic titanites.
— Double underlining = considered realistic in these samples.
— Single underlining = considered doubtful in these samples.
— Not underlined = not detected in these samples.
— *Italics* = hypothesis excluded in these samples.

Kienast, 1987; Perseil, 1985, 1987, 1988, 1991). These manganese concentrations were subsequently penetrated by several networks of cross-cutting veins and late fractures which were responsible for the mobilization of certain elements, in particular K, Sr and Ba. Further details on the petrological, metallogenical and geochemical environments are provided in the thesis of Martin-Vernizzi (1982), the review of Mottana (1986) and the above-cited references.

Dufrenoy (1847) recorded an Mn-rich titanite named 'greenovite' (2.90–3.80 wt.% MnO) collected by de Lom (1843) from the St. Marcel-Praborna locality. Fermor (1908) also mentioned 'greenovite' in gondites from India. In a more modern study with an electron microprobe on greenovites from St. Marcel-Praborna, Mottana and Griffin (1979) recorded Mn contents only slightly higher than trace values: 0.39–0.99 wt.% MnO) and they suspected that the older analyses may have been 'contaminated with braunite or another Mn phase'. We support the contamination hypothesis as we have often observed minute inclusions of Sr-bearing piemontite and of braunite in microfractures in pink titanites from St. Marcel-Praborna which Dufrenoy (1847) and other workers during that epoch would not have been able to avoid in bulk-mineral analyses. Mottana and Griffin (1979) deduced that the Mn was most probably divalent and situated in the Ca site.

In this work, petrographical and crystal-chemical details are presented of our discovery of Mn-bearing (0.00–0.51 wt.% Mn_2O_3) Sb-rich titanite in three different petrographical environments at the St. Marcel-Praborna locality. Table 1 lists all of the known chemical elements which can substitute into the titanite structure, ideally $CaTiOSiO_4$ (Zachariasen, 1930), as mentioned in the reviews by Sahama (1946), Ribbe (1980), Deer *et al.* (1982), Smith (1988) and Oberti *et al.* (1991), and now adds antimony to the list.

Petrographical notes

Three petrographical environments

I The Emerald-Green Horizon. This term (Martin-Vernizzi, 1982) defined a green pyroxene-bearing feldspathic quartzite cut by numerous feldspathic cm-sized veins. The colour derives from the presence of zoned green pyroxenes of aegirine-bearing augite composition with variable contents of Cr, Mn and Fe. The Sb-rich titanite here is accompanied by large crystals of albite, calcite, green amphibole, and green chlorite, all of which are compatible with a greenschist-facies assemblage. There are no Mn-oxides associated with titanite here, but the latter crystals, which often exceed several hundreds of μm in size, are rich in inclusions of Sr-bearing piemontite, Sb-free rutile needles and Cr-bearing magnetite (hematite lamellae transformed into magnetite) (Fig. 1).

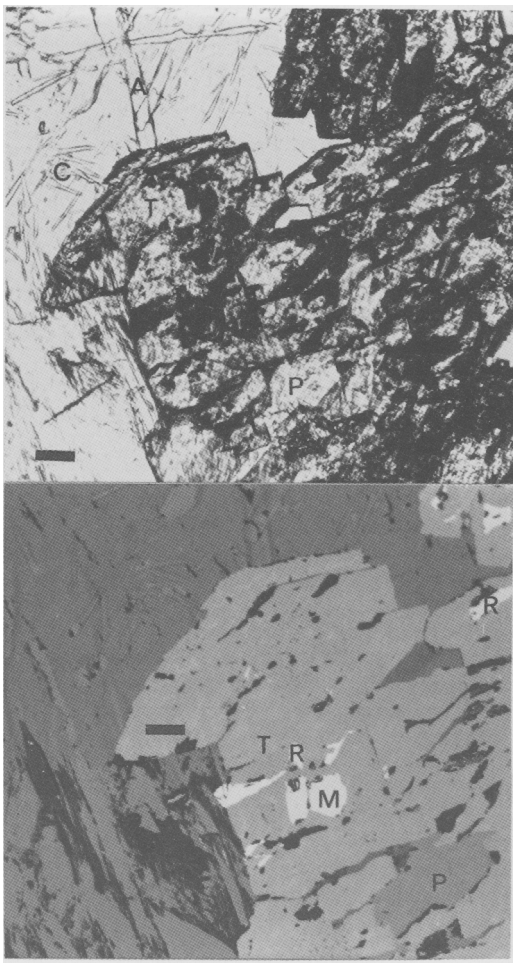

FIG. 1. Sb-rich titanite adjacent to a microfissure containing green amphibole (A) and green chlorite (C) from the 'emerald-green horizon' (environment I). Black scale bars = 50 μm. (*a*) Plane polarized light image revealing typical Sb-rich titanite (T) rich in inclusions of opaque oxides and of piemontite (P) of lower refractive index and strong pleochroism. (*b*) Reflected light image permitting a better distinction between the inclusions of piemontite (P, dark grey), elongated grains of rutile (R, white), and irregular grains of hematite pseudomorphed by magnetite (M, white). The two oxides of similar reflectance can be distinguished by the anisotropy of the rutile compared to the almost isotropic nature of the magnetite.

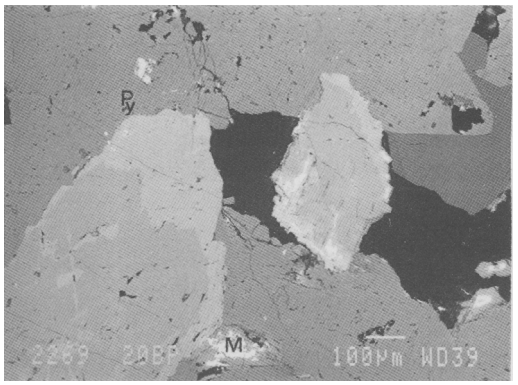

FIG. 2. SEM image of two zoned Sb-rich titanite grains from the same 'emerald-green horizon'. The brighter intensities, indicating a higher mean atomic number (principally Sb but also Fe), are essentially confined to the grain boundaries but occasionally occur within the core. These titanites are surrounded by green pyroxene (Py), an aegirine-augite rich in Cr and containing inclusions of martitized magnetite (M).

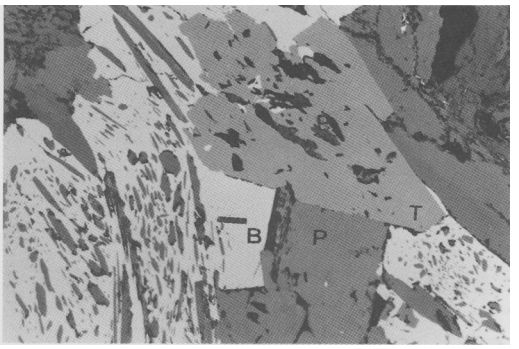

FIG. 3. Reflected light image of a 'cm-sized late veinlet' (environment II). The Sb-rich titanites (T) contain some inclusions of braunite (light grey) and of Sr-bearing piemontite (P, medium grey). The larger grains of braunite (B) are very rich in elongated inclusions of richterite (dark grey) and Mn-bearing phengite (light grey). Independent grains of Sr-bearing piemontite (P) also occur. Black scale bar = 50 µm.

Back-scattered electron images of the titanites reveal significant zoning (Fig. 2); the brightest parts corresponding to the highest mean atomic number are the Sb-richest parts which also contain substantial Cr contents (see below), the latter point correlating with the Cr content of the magnetites.

II Late-stage cm-sized veinlets. These veinlets, which seem to cross-cut horizon I in the loose fragments collected (but this is never clearly observed in the field), are composed of quartz, albite, hematite, Mn-bearing tremolite, Sr-bearing piemontite, Fe-bearing braunite and Sb-rich titanite (Fig. 3). These veins are in fact characterized by the Fe-rich nature of the braunite in which Fe can replace up to 10% of the Mn, in contrast to all the other braunite occurrences, Fe-poor, at this locality (Perseil, 1985). These braunites contain abundant voluminous inclusions of Mn- and Fe-bearing richterite, and the grains of zoned Sb-rich titanite contain inclusions of hematite, Sr-bearing piemontite, braunite and Sb-free rutile (Fig. 3). Hollandite also occurs in mm-sized veinlets (not those of environment III) found very close to these cm-sized veinlets.

The host rock is an amphibole-rich dark-grey-green amphibolite.

III Microfissured late-stage mm-sized veinlets. These veinlets, also collected in loose blocks, are not the same as those of type II since they differ in micropetrography and microstructure. Petrographically they differ in having a porous aspect, skeleton-shaped crystals of Sr-bearing piemontite (up to 7 wt.% SrO) containing cores of albite or of pyroxene, and stacks of Mn-bearing phengite (up to 2.6 wt.% MnO), whereas they are similar in containing quartz, hematite and Sb-rich titanite.

The titanites are again chemically zoned, but they are also penetrated by a network of microfractures which can best be observed with a scanning electron microscope (Fig. 4), but also sometimes with an ordinary petrological microscope (Fig. 5). The Sb-richest parts occur at the grain boundaries and alongside fractures, pores or inclusions, thus indicating a very late mobilization and penetrative metasomatism by Sb. The inclusions are either of Sb-rich rutile (up to 36.05 wt.% Sb_2O_5 = 0.22 Sb per O = 2.00; Smith and Perseil, in prep.), or of mica having chemical compositions close to those of Mn-bearing phlogopite which occurs in the matrix, or of roméite (E.-A.Perseil, unpub. data). The Sb-rich titanites also contain noticeable contents of Sr (see below).

The host rock is an albite-rich light-grey-green amphibolite also rich in magnetite (mostly oxidized to hematite).

Other environments

Titanite is known from other petrographical environments within the basal quartzite unit, but the Sb content is either non-determined or insignificant: all the other elements in the Ti site together constitute less than 10 cation % of impurities in the analysed crystals which are therefore relatively pure $CaTiOSiO_4$ (cf. Mottana and Griffin, 1979; Martin-Vernizzi, 1982: E.-A.Perseil, unpub. data).

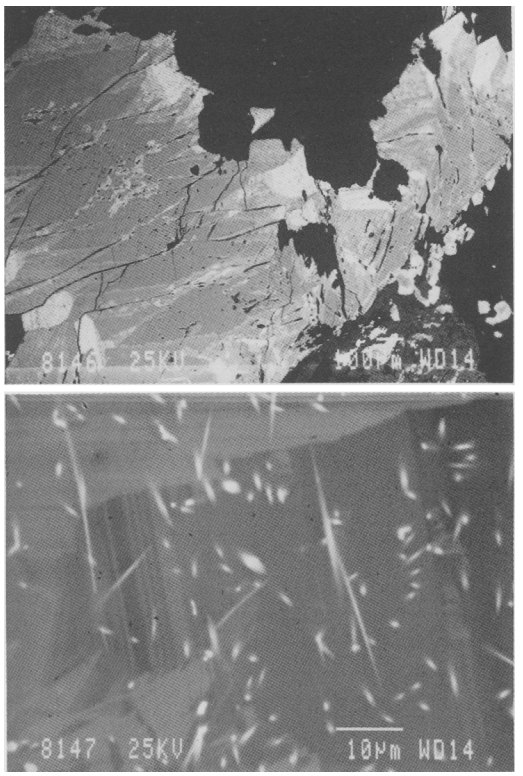

FIG. 4. SEM images of an Sb-rich titanite from a 'microfissured mm-sized late veinlet' (environment III). (*a*) Vast network of inclusions, microfissures and pores. The brightest parts richest in Sb (and Fe) are again distributed at the grain boundaries but also alongside the inclusions, microfractures and pores. (*b*) Close up of a medium-gray twinned grain boundary of Fig. 4*a* showing needle- or oval-shaped grains of rutile (white) much richer in Sb than the brighter zones of Sb-rich titanite of Fig. 4*a*.

Mineralogical markers of chemical mobility

Apart from the different structural and petrographical features of each of the three environments of Sb-rich titanite, several chemical fingerprints also serve to distinguish them:

I — notable Cr in magnetite; Cr-richest titanite;
II — notable Fe in braunite; Cr-free, Ba-free, F-free titanite;
III — notable Sb in rutile; Sr-richest titanite.

On the other hand some other properties are common, such as the Sr-bearing nature of the piemontite in each environment. As will be seen below the titanites also contain Sr, Ba, Al, Cr, Mn,

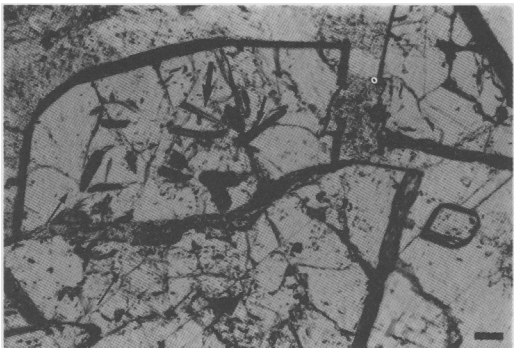

FIG. 5. Elongate inclusions of Sb-rich rutile (thick arrows) within a fractured grain of Sb-rich titanite (centre and bottom) from a 'microfissured mm-sized late veinlet' (environment III). Minute equant inclusions of roméite (thin arrows) occur close to microfissures. Plane polarized light. Black scale bar = 10 μm.

Fe, (OH) and F in addition to Ca, Ti, Sb, Si and O such that a large number of elements were available at the locality. The recorded enrichments in Na, K, Sr and/or Ba of various minerals in the basal quartzite unit are always related to a network of fissures (e.g. Martin-Vernizzi, 1982; Perseil, 1985, 1988; Mottana, 1986; Martin and Kienast, 1987). However it is emphasized that the Mn-bearing and variable f_{O_2} natures of the manganese concentrations were pre-eclogite features, although some Mn and/or O may well have been remobilized subsequently.

The growth of the titanites in the veinlets (environments II and III) was obviously a syn-veinlet event. The growth of the titanites in the 'Emerald Green Horizon' is of uncertain age: possibly syn-eclogite but more probably post-eclogite pre-veinlet, or both syn- and post-eclogite; however one cannot exclude syn-veinlet neoblastic growth of the titanites in this horizon.

One key question is whether the mobile Sb replaced Ti in pre-existing titanite grains or if the Sb-rich titanite zones represent later overgrowths. Whereas the images in Fig. 2 for environment I are compatible with either hypothesis, the images in Fig. 4 for environment III support a very late influx of Sb replacing Ti, i.e. later than the developent of the microfissured veinlets, and hence one of the latest geological/geochemical events at this locality. Since the same chemical process occurred in the Sb-rich rutile microinclusions within the same titanite crystals in environment III (Smith and Perseil, in prep.), it seems obvious that the two processes of 'antimonization' of titanite and of rutile were contemporaneous. The 'antimonization' of

the titanites in environments I and II most probably occurred at the same time, although this cannot yet be proved.

Another key question concerns what happened to the Ti atoms displaced by the Sb atoms. One could imagine that they migrated to the borders of the titanite crystals and there they were fixed in a narrow overgrowth zone of neoblastic Sb-rich titanite rich in Sb because of the external source of Sb. In this case some of the outermost parts of the zoned titanite crystals might be of later age of first crystallization than the inner parts, as suggested above (i.e. the processes of metasomatism and of overgrowths both occurred).

There is however an attractive alternative hypothesis whereby the expelled Ti migrated further into the matrix. In this connection it is interesting to note that new data (E.-A. Perseil, unpub. data) on the somewhat fuzzy very-fine-grained 'filigrane' type of braunite described by Perseil (1985) indicate that the outermost parts, which petrographically seem to be of very late age, are richer in Ti than previously reported analyses (up to 0.315 Ti per O = 12). Likewise some hollandites contain up to 0.21 Ti per O = 16. Nevertheless these new data come from environment II only.

In contrast one could argue that the expelled Ti migrated very little and in fact created the Sb-rich rutiles at this late stage; this hypothesis has the advantage of explaining why the rutile microinclusions exist where they do within the Sb-rich titanites, but this does not explain their occurrence within the Sr-bearing piemontites (Perseil, 1991) (see Smith and Perseil, in prep., for a detailed discussion). In any case Ti must be added to the list of elements mobile at a very late stage.

It is interesting to note that Au was also discovered in the 'Emerald Green Horizon' by Millosevich (1906) and Colomba (1910) and that Sb is often intimately associated with Au (Rota and Hausen, 1991; Maury *et al.*, 1993). It is thus quite likely that Au also occurs in environments II and III. If so then Sb-rich titanite could be a chemical marker for Au like Sn-rich titanite is for W mineralizations (Gibert *et al.*, 1990).

Mineral chemistry

Analytical methods

The rocks were mounted in polished thin sections and were examined with transmitted and reflected light microscopy, and scanning electron microscopy (SEM) with backscattered electron images.

The minerals were analysed with the CAMEBAX electron microprobe (EMP) at the Muséum National d'Histoire Naturelle, Paris, under the operating conditions: 15 kV, 10 nA, 6 s integration time. Other analytical conditions, including the standards and the analytical precision are quoted in Table 2. Several other elements (in particular Na, Mg, P, Cl, Zr, Nb, Sn, *REE*, Ta and Pb) were included in the EMP programme or were searched for with an energy-dispersive detector attached to the SEM, but all were either not detected or gave values less than 0.01 wt.% oxide and were henceforth ignored.

The EMP analyses are presented, in order of increasing TiO_2, separately for the three petrographical environments in Tables 3–5 respectively. Each listed analysis represents around twenty nearly-identical point analyses. The analysis no. 6 in Table 3 is accompanied by its standard deviation (one sigma; $n = 19$) for each oxide and these values are taken as being representative for all the listed analyses. When examining the corresponding cation plots, the $\pm$ two sigma uncertainty limits should indicate the maximum uncertainty for around 95% of the data values, e.g. $\pm$ 0.010 Sb^{5+} for all but one of the twenty listed analyses.

Crystal-chemistry: 1

Valencies, co-ordinations and substitutions

Table 1 summarizes the numerous possibilities of valencies and/or co-ordinations for all the mentioned elements, notably for the transition metals (period 4) Sc, Ti, V, Cr, Mn, Fe and Cu, the group 5B elements V, Nb and Ta, the group 5A elements Sb and Bi and the actinides Th and U. Some of the valencies listed are unusual for geologists but are known by chemists. The ranges of valencies, co-ordinations and ionic radii listed, coupled with chemical affinities indicated by the Periodic Table, permit several predictions of other elements which ought to be able to enter the titanite structure but which apparently have not yet been recorded (e.g. Co, As, Hf...).

The attribution of valencies and of site co-ordinations for the analysed elements is unequivocal for $^{vii}Ca^{2+}$, $^{vii}Sr^{2+}$, $^{vii}Ba^{2+}$, $^{iv}Si^{4+}$, $^{O1-O5}O^{2-}$, $^{O1}OH^{-}$ and $^{O1}F^{-}$. O1–O5 indicate the oxygen positions in relation to Ti. The strongly-reducing cations Cr^{2+} and Ti^{3+} may be excluded on the basis of the highly oxidized nature of many minerals in the rocks concerned (although the replacement of hematite by Cr-bearing magnetite in environment I indicates a reduction process).

In the Ca site, trivalent $^{vii}Cr^{3+}$, $^{vii}Mn^{3+}$ and $^{vii}Fe^{3+}$ are rather small whereas divalent $^{vii}Mn^{2+}$ and $^{vii}Fe^{2+}$ are as close in size to $^{vii}Ca^{2+}$ as are the listed heavier elements $^{vii}Sr^{2+}$ and $^{vii}Ba^{2+}$. Hence the principal substitution concerning this site is deduced to be simply the homovalent one:

TABLE 2. Electron microprobe analytical conditions

Element	Crystal	X-ray Line	Analytical precision (%) on oxide	Standard
Ca	PET	Kα1	0.2	wollastonite
Sr	TAP	Lα1	0.3	strontianite
Ba	LiF	Lα1	0.3	baryte
Ti	LiF	Kα1	0.3	rutile
Al	TAP	Kα1	0.1	Al_2O_3 (synthetic)
Cr	PET	Kα1	0.1	Cr_2O_3 (synthetic)
Mn	LiF	Kα1	0.2	rhodonite
Fe	LiF	Kα1	0.2	hematite
Sb	PET	Kα1	0.2	Sb (metal)
Si	TAP	Lα1	0.2	wollastonite
F	TAP	Kα1	0.7	apatite

$$^{vii}R^{2+} = {}^{vii}R^{2+} \quad (1)$$

i.e.

$$^{vii}Ca^{2+} = {}^{vii}[Sr^{2+} + Ba^{2+} + Mn^{2+} + Fe^{2+}] \quad (2)$$

However trivalent Sb may also be possible by means of the heterovalent unbalanced substitution:

$$^{vii}R^{2+} = {}^{vii}R^{3+} + e^- \quad (3)$$

i.e.

$$^{vii}Ca^{2+} = {}^{vii}Sb^{3+} + e^- \quad (4)$$

which is analogous to trivalent REE substitution in certain high-temperature titanites. Tetravalent cations are not indicated in these samples but they should exist in metamict titanites as the ionic radius of Th^{4+} is better suited to co-ordination VII (e.g. Černý and Povondra, 1972); this would cause a double charge change:

$$^{vii}R^{2+} = {}^{vii}R^{4+} + 2\ e^- \quad (5)$$

The monovalent substitution

$$^{vii}R^{2+} = {}^{vii}R^{+} - e^- \quad (6)$$

which must occur in Na-bearing titanites, does not occur significantly at St. Marcel-Praborna as Na occurs only in trace quantities.

In the Si site, there is no evidence for $4 \times {}^{iv}H^+$ in these samples, although it would provide a convenient way to fill up the Si site where necessary, i.e. most formulae calculated by method (*f*) or (*g*) (see p. 727). The substitutions

$$^{iv}R^{4+} = {}^{iv}R^{3+} - e^- \quad (7)$$

e.g.

$$^{iv}Si^{4+} = {}^{iv}Al^{3+} - e^- \quad (8)$$

or

$$^{iv}R^{4+} = {}^{iv}R^{4+} \quad (9)$$

e.g.

$$^{iv}Si^{4+} = {}^{iv}Ti^{4+} \quad (10)$$

are somewhat doubtful at St. Marcel-Praborna since these large cations require relatively low-*P*–high-*T* conditions in titanite (e.g. Oberti *et al.*, 1991) and in many other aluminosilicate minerals, notably amphiboles and pyroxenes (e.g. Smith, 1988).

The same *P*–*T*-size effect probably also concerns to a greater degree the transition elements V, Cr, Mn and Fe of diverse valencies but mostly of even larger ionic radius. Since P and V are lacking in these samples, the pentavalent substitution:

$$^{iv}R^{4+} = {}^{iv}R^{5+} + e^- \quad (11)$$

does not occur

In the O1 site, where O1 indicates the special oxygen position linking the octahedra of the Ti site which is crystallographically quite distinct from the other four oxygens of the tetrahedra of the Si site (Zachariasen, 1930), the heterovalent substitution:

$$^{O1}R^{2-} = {}^{O1}R^{-} + e^- \quad (12)$$

i.e.

$$^{O1}O^{2-} = {}^{O1}[F^- + OH^-] + e^- \quad (13)$$

is well-known in Nature (and in high *P*–*T* experiments where it is coupled with the Al^{3+} component of substitution (18): e.g. Smith, 1981, 1988); it occurs to some extent at St. Marcel-Praborna (very minor for F^- and unknown but expected for OH^-).

In the Ti site, a large number of chemical substitutions of the types:

$$^{vi}R^{4+} = {}^{vi}R^{3+} - e^- \quad (14)$$

TABLE 3. EMP analyses of Sb-rich titanite from environment I

The Emerald Green Horizon

	1	2	3	4	5	6	σ
CaO	25.93	25.68	26.36	25.73	26.48	26.03	0.34
SrO	0.42	0.45	0.44	0.36	0.11	0.37	0.10
BaO	0.44	0.02	0.37	0.00	0.34	0.10	0.17
TiO_2	28.79	31.90	33.04	34.01	35.08	28.34	0.59
Al_2O_3	0.60	0.54	0.97	0.89	0.37	1.22	0.07
Cr_2O_3	2.39	2.18	0.62	1.06	1.03	1.00	0.08
Mn_2O_3	0.02	0.17	0.22	0.24	0.00	0.20	0.09
Fe_2O_3	1.23	1.23	1.81	1.66	1.70	2.21	0.22
Sb_2O_5	10.57	7.85	5.89	6.38	4.05	9.93	0.40
SiO_2	28.73	28.54	28.72	28.28	28.96	28.90	0.35
F	0.00	0.00	0.16	0.02	0.16	0.12	0.11
Total	99.12	98.56	98.60	98.63	98.28	98.42	
Structural formulae by method (*g*): Σ(vii+vi+iv) = 3							
Cations							
Ca^{2+}	0.969	0.953	0.968	0.947	0.968	0.972	0.013
Sr^{2+}	0.008	0.009	0.009	0.007	0.002	0.007	0.002
Ba^{2+}	0.006	0.000	0.005	0.000	0.005	0.001	0.002
Σ(vii)	0.983	0.962	0.981	0.954	0.975	0.981	0.013
Ti^{4+}	0.755	0.831	0.851	0.879	0.900	0.743	0.015
Al^{3+}	0.025	0.022	0.039	0.036	0.015	0.050	0.003
Cr^{3+}	0.066	0.060	0.017	0.029	0.028	0.028	0.002
Mn^{3+}	0.001	0.004	0.006	0.006	0.000	0.005	0.002
Fe^{3+}	0.032	0.032	0.047	0.043	0.044	0.058	0.006
$\Sigma(R^{3+})$	0.123	0.118	0.108	0.114	0.086	0.141	0.007
Sb^{5+}	0.137	0.101	0.075	0.081	0.051	0.129	0.005
Σ(vi)	1.015	1.050	1.035	1.074	1.038	1.012	0.018
Si^{4+}	1.002	0.988	0.984	0.972	0.988	1.007	0.012
Σ(iv)	1.002	0.988	0.984	0.972	0.988	1.007	0.012
Σ(vi+iv)	2.017	2.038	2.019	2.046	2.026	2.019	0.022
Σ(cations)	3.000	3.000	3.000	3.000	3.000	3.000	0.025
Σ(charge)	10.047	10.059	9.987	10.057	9.999	10.013	
Anions							
F^-	0.000	0.000	0.017	0.002	0.017	0.013	0.012
OH^-(calc)	−0.047	−0.059	−0.004	−0.059	−0.016	−0.026	
(F+OH)	−0.047	−0.059	0.013	−0.057	0.001	−0.013	
O^{2-}(calc)	5.047	5.059	4.987	5.057	4.999	5.013	
Σ(anions)	5.000	5.000	5.000	5.000	5.000	5.000	

$$^{vi}R^{4+} = {}^{vi}R^{4+} \quad (15)$$

$$^{vi}R^{4+} = {}^{vi}R^{5+} + e^- \quad (16)$$

have already been recorded (see references below), but one can also consider the double charge change:

$$^{vi}R^{4+} = {}^{vi}R^{2+} - 2e^- \quad (17)$$

for example to introduce $^{vi}Mn^{2+}$ or $^{vi}Fe^{2+}$.

Highly-charged pentavalent $^{vi}Cr^{5+}$ and tetravalent $^{vi}Cr^{4+}$ and $^{vi}Mn^{4+}$ are slightly smaller than $^{vi}Ti^{4+}$, whereas trivalent $^{vi}Cr^{3+}$, $^{vi}Mn^{3+}$ and $^{vi}Fe^{3+}$ are slightly larger than, but even closer to, $^{vi}Ti^{4+}$. The divalent transition elements $^{vi}Mn^{2+}$ and $^{vi}Fe^{2+}$ are rather large. Thus trivalent Cr, Mn and Fe in the Ti site are considered the most reasonable solutions, but it must be remembered that two types of valency and

TABLE 4. EMP analyses of Sb-rich titanite from environment II

Late-stage veinlets

	1	2	3	4	5	6	7
CaO	26.41	26.83	26.12	27.14	26.99	27.04	27.81
SrO	0.45	0.26	0.18	0.07	0.17	0.15	0.00
BaO	0.00	0.00	0.00	0.00	0.00	0.00	0.00
TiO_2	31.46	33.78	35.08	35.21	35.55	36.47	38.44
Al_2O_3	1.34	1.50	1.05	1.19	1.26	0.94	0.65
Cr_2O_3	0.00	0.00	0.00	0.00	0.00	0.00	0.00
Mn_2O_3	0.37	0.29	0.38	0.23	0.30	0.33	0.51
Fe_2O	2.38	2.24	1.72	2.00	1.61	1.04	0.38
Sb_2O_5	7.13	4.92	5.09	3.33	3.80	3.37	0.71
SiO_2	28.51	28.43	28.68	29.16	29.02	29.20	29.71
F	0.00	0.00	0.00	0.00	0.00	0.00	0.00
Total	98.05	98.25	98.30	98.33	98.70	98.54	98.21
Structural formulae by method (*g*): Σ(vii+vi+iv) = 3							
Cations							
Ca^{2+}	0.975	0.977	0.956	0.979	0.974	0.976	0.992
Sr^{2+}	0.009	0.005	0.004	0.001	0.003	0.003	0.000
Ba^{2+}	0.000	0.000	0.000	0.000	0.000	0.000	0.000
Σ(vii)	0.984	0.983	0.959	0.981	0.977	0.979	0.992
Ti^{4+}	0.816	0.864	0.901	0.892	0.900	0.924	0.962
Al^{3+}	0.054	0.060	0.042	0.047	0.050	0.037	0.026
Cr^{3+}	0.000	0.000	0.000	0.000	0.000	0.000	0.000
Mn^{3+}	0.010	0.008	0.010	0.006	0.008	0.008	0.013
Fe^{3+}	0.062	0.057	0.044	0.051	0.041	0.026	0.010
$\Sigma(R^{3+})$	0.126	0.125	0.096	0.104	0.098	0.072	0.048
Sb^{5+}	0.091	0.062	0.065	0.042	0.048	0.042	0.009
Σ(vi)	1.033	1.051	1.062	1.037	1.046	1.038	1.019
Si^{4+}	0.983	0.967	0.979	0.982	0.977	0.983	0.989
Σ(iv)	0.983	0.967	0.979	0.982	0.977	0.983	0.989
Σ(vi+iv)	2.016	2.017	2.041	2.019	2.023	2.021	2.008
Σ(cations)	3.000	3.000	3.000	3.000	3.000	3.000	3.000
Σ(charge)	9.997	9.972	10.050	9.976	9.995	10.013	9.977
Anions							
F^-	0.000	0.000	0.000	0.000	0.000	0.000	0.000
OH^-(calc)	0.003	0.028	−0.050	0.024	0.005	−0.013	0.023
(F+OH)	0.003	0.028	−0.050	0.024	0.005	−0.013	0.023
O^{2-}(calc)	4.997	4.972	5.050	4.976	4.995	5.013	4.977
Σ(anions)	5.000	5.000	5.000	5.000	5.000	5.000	5.000

co-ordination may be present simultaneously, e.g. divalent Fe and trivalent Fe respectively in the Ca and Ti sites (cf. in the different sites *M*1, *M*2, *M*3 and *M*4 in 'iron'-, 'ferro-' and/or 'ferri-' amphiboles). Since our data-set does not permit definitive choices, Cr, Mn and Fe are all provisionally attributed to valency 3 only, along with $^{vi}Al^{3+}$, in the Ti site only by substitution (14), i.e.

$$^{vi}Ti^{4+} = {}^{vi}[Al^{3+} + Cr^{3+} + Mn^{3+} + Fe^{3+}] - e^- \quad (18)$$

$^{vi}Sb^{3+}$ is rather large for the Ti site but is smaller than $^{vi}Fe^{2+}$ which is sometimes attributed to the Ti site; thus Sb could join the other R^{3+} cations by substitution (14):

$$^{vi}Ti^{4+} = {}^{vi}Sb^{3+} - e^- \quad (19)$$

Substitution (16) with R^{5+} has already been invoked for the group 5B metals, e.g. $^{vi}V^{5+}$ (Bernau and Franz, 1987), $^{vi}Nb^{5+}$ (Paul *et al.*, 1981; Russell *et al.*, 1994), and $^{vi}Ta^{5+}$ (Clark, 1974; Groat *et al.*,

TABLE 5. EMP analyses of Sb-rich titanite from environment III

Microfissured late-stage veinlets

	1	2	3	4	5	6	7
CaO	25.02	24.68	25.25	24.52	24.48	25.08	26.89
SrO	0.76	0.84	0.54	0.65	0.74	0.51	0.35
BaO	0.00	0.06	0.13	0.35	0.06	0.49	0.24
TiO_2	26.18	28.37	28.69	28.86	29.23	31.65	34.42
Al_2O_3	2.31	2.03	2.12	1.99	2.10	1.68	1.51
Cr_2O_3	0.10	0.19	0.00	0.02	0.00	0.07	0.14
Mn_2O_3	0.30	0.33	0.26	0.21	0.23	0.33	0.07
Fe_2O_3	2.80	3.00	2.41	2.81	2.51	2.21	1.40
Sb_2O_5	12.59	12.38	10.92	11.98	11.64	9.29	4.63
SiO_2	28.33	28.44	28.69	28.41	28.42	28.13	30.08
F	0.00	0.17	0.12	0.22	0.09	0.12	0.00
Total	98.39	100.49	99.13	100.02	99.50	99.56	99.73
Structural formulae by method (*g*): Σ(vii+vi+iv) = 3							
Cations							
Ca^{2+}	0.945	0.918	0.941	0.917	0.916	0.930	0.963
Sr^{2+}	0.016	0.017	0.011	0.013	0.015	0.010	0.007
Ba^{2+}	0.000	0.001	0.002	0.005	0.001	0.007	0.003
Σ(vii)	0.961	0.936	0.954	0.935	0.931	0.947	0.973
Ti^{4+}	0.694	0.741	0.750	0.757	0.767	0.824	0.865
Al^{3+}	0.096	0.083	0.087	0.082	0.086	0.069	0.059
Cr^{3+}	0.003	0.005	0.000	0.001	0.000	0.002	0.004
Mn^{3+}	0.008	0.009	0.007	0.006	0.006	0.009	0.002
Fe^{3+}	0.074	0.078	0.063	0.074	0.066	0.058	0.035
$\Sigma(R^{3+})$	0.181	0.175	0.157	0.162	0.158	0.137	0.100
Sb^{5+}	0.165	0.160	0.141	0.155	0.151	0.119	0.057
Σ(vi)	1.040	1.076	1.048	1.074	1.077	1.080	1.022
Si^{4+}	0.999	0.988	0.998	0.991	0.992	0.973	1.005
Σ(iv)	0.999	0.988	0.998	0.991	0.992	0.973	1.005
Σ(vi+iv)	2.039	2.064	2.046	2.065	2.069	2.053	2.027
Σ(cations)	3.000	3.000	3.000	3.000	3.000	3.000	3.000
Σ(charge)	10.062	10.093	10.064	10.100	10.120	10.076	10.012
Anions							
F^-	0.000	0.019	0.013	0.024	0.010	0.013	0.000
OH^-(calc)	−0.062	−0.112	−0.077	−0.124	−0.130	−0.089	−0.012
(F+OH)	−0.062	−0.093	−0.064	−0.100	−0.120	−0.076	−0.012
O^{2-}(calc)	5.062	5.093	5.064	5.100	5.120	5.076	5.012
Σ(anions)	5.000	5.000	5.000	5.000	5.000	5.000	5.000

1985), although Bernau and Franz (1987) discussed at length the alternative possibilities of valencies 3+ and 4+ for vanadium. At St. Marcel-Praborna the analogous substitution would be

$$^{vi}Ti^{4+} = {}^{vi}Sb^{5+} + e^- \qquad (20)$$

and this is strongly supported by the fact that $^{vi}Sb^{5+}$ has the same ionic radius as $^{vi}Ti^{4+}$. The latter point thus favours the operation of substitution (20) over that of (19). Pentavalent Sb is known in several compounds, e.g. $NaSbO_3$ and $FeSbO_4$ (Heslop and Robinson, 1963, p. 350), as well as in the natural minerals swedenborgite ($NaBe_4SbO_7$) and (Mn,Fe,Sb)-bearing rutile (Smith and Perseil, in prep.). For all these reasons the valency 5+ was used for antimony instead of 3+ in Tables 3–5. However this does not exclude the possibility that some of the Sb may be trivalent, as in the natural mineral valentinite (Sb_2O_3).

Since it is not unknown in natural minerals to find the same chemical element with two different valencies in the same site (e.g. Mn^{3+} as well as

Mn^{4+} in the manjiroite–cryptomelane–hollandite–coronadite series $(Na,K,Ba,Pb)Mn_8O_{16}$), cf. Post and Bish, 1989), then it is possible that Sb occurs in the Ti site as both $^{vi}Sb^{3+}$ and $^{vi}Sb^{5+}$. This would have the important consequence of tending to eliminate the need for another ionic exchange, such as (3), (5), (6), (7) or (12), in order to balance the charges of substitutions (14) or (16), since the principal substitution could be:

$$2\ ^{vi}Ti^{4+} = {}^{vi}Sb^{3+} + {}^{vi}Sb^{5+} \quad (21)$$

which is the sum of substitutions (19) and (20), i.e.

$$2\ ^{vi}R^{4+} = {}^{vi}R^{3+} + {}^{vi}R^{5+} \quad (22)$$

which of course is merely the sum of substitutions (14) and (16).

The combination of substitutions (18) and (20) gives:

$$2\ ^{vi}Ti^{4+} = {}^{vi}[Al^{3+} + Cr^{3+} + Mn^{3+} + Fe^{3+}] + {}^{vi}Sb^{5+} \quad (23)$$

which is exactly the same substitution as demonstrated in Sb-rich rutiles at St. Marcel-Praborna (Smith and Perseil, in prep.). Furthermore, this overall isovalent coupled substitution (22) has been deduced by most of the above-mentioned workers on pentavalent V, Nb and Ta.

These various equations can of course be combined in numerous ways, balancing charges where necessary with two or more of the several heterovalent substitutions mentioned in one or other of the four ion sites. For example, combining equations (4) and (8) leads to:

$$^{vii}Ca^{2+} + {}^{iv}Si^{4+} = {}^{vii}Sb^{3+} + {}^{iv}Al^{3+} \quad (24)$$

and combining equations (13) and (19) leads to

$$^{vi}Ti^{4+} + {}^{O1}O^{2-} = {}^{vi}Sb^{3+} + {}^{O1}[F^- + OH^-] \quad (25)$$

which is the Sb-equivalent of the Al-substitution common in eclogite-facies rocks (Smith, 1981, 1988). The only essential criterion being that of overall charge balance, the choice of equations to combine is largely subjective and hence is not pursued further here except to emphasize that the substitution (23) is considered dominant because of both the excellent credibility of its component substitutions (18) and (20) and the substantial quantities of R^{3+} and Sb^{5+} in these samples.

Pascal (1958, p. 527) and Heslop and Robinson (1963, p. 344) stated that the essential valencies of Sb are 3+ and 5+ (amongst known valencies from 3− to 5+), but they also emphasized the strong covalent nature of much of the bonding of this semi-metal such that any purely ionic notation is imprecise. Sb^{4+} may thus be no less precise and it is indicated in the solid state in antimony tetroxide Sb_2O_4 (Pascal, 1958). One could thus imagine the homovalent substitution (15), i.e.

$$^{vi}Ti^{4+} = {}^{vi}Sb^{4+} \quad (26)$$

which is well accepted for the substitution of, for example, $^{vi}Sn^{4+}$ or $^{vi}Zr^{4+}$ in the titanite structure. Tetravalent Sb is set aside here (cf. $^{vi}Cr^{4+}$ and $^{vi}Mn^{4+}$ above) in favour of substitution (21), but these tetravalent states are not ruled out entirely.

Crystal-chemistry: 2

Cation/anion sums and mineral stoichiometry

Calculating the structural formulae of titanites is always difficult since no cation or anion value is fixed. Since (OH) and/or F are frequently present in variable amounts in titanites of diverse origins, and since one or both of these anions are usually not determined, then it is impossible to calculate on any anion basis, such as constant O^{2-}, constant $(OH,F)^-$ or constant charge. Where this has been done in the literature, the results have very often led to unacceptably high or low cation values, especially site overpopulations. Thus most authors now calculate on a basis of constant cations although this sometimes necessitates that there are no cation vacancies. Although this is reasonable for the iv- and vi-co-ordinated sites, it is not so obviously valid for the vii-co-ordinated site. Furthermore since all possible elements are generally not determined, then small 'apparent vacancies' ought to arise when non-analysed elements are really present. Worse still is the fact that calculating to a constant cation sum in one site often leads to an overpopulation of a different site which is crystallographically untenable; e.g. fixing Ca = 1.0 often leads to Si > 1.0.

Setting aside temporarily both valencies and co-ordinations, there are seven principal ways of fixing the cation sums:

(*a*) sum ^{vii} = 1.0 (cf. Oberti *et al.*, 1991, if Si < = 1.0);
(*b*) sum ^{vi} = 1.0;
(*c*) sum ^{iv} = 1.0 (cf. Mottana and Griffin, 1979; Paul *et al.*, 1981; Deer *et al.*, 1982);
(*d*) sum $^{(vii + vi)}$ = 2.0;
(*e*) sum $^{(vii + iv)}$ = 2.0;
(*f*) sum $^{(vi + iv)}$ = 2.0 (cf. Paul *et al.*, 1981; Oberti *et al.*, 1991); and
(*g*) sum $^{(vii + vi + iv)}$ = 3.0 (cf. Groat *et al.*, 1985; Bernau and Franz, 1987).

The uncertainties over the valencies of Cr, Mn, Fe and especially Sb, as well as the possible presence of more than one valency simultaneously for the same element, permit many possible combinations for constructing structural formulae. The uncertainties over the site co-ordinations for Mn, Fe, Sb, Al and Ti

create so many further permutations that the problem is quite insoluble. Here in Tables 3–5 we present the data calculated according to one fixed method which seems better than most: method (g); with valencies chosen initially as trivalent only for Cr, Mn and Fe, and pentavalent only for Sb; co-ordinations chosen initially as vii for all divalent cations, vi for all the trivalent cations, Ti^{4+} and Sb^{5+}, and iv for Si^{4+} alone. After commenting on the consequent cation or anion sums, with suggestions on how to alleviate problems by adjusting valencies or co-ordinations, we proceed to comment on the positive or negative effects of the other six constant cation calculation methods since few authors actually discuss their relative merits, and even fewer actually publish the values of several crystallographically-critical parameters, such as total charge or site occupancies, which might demonstrate the inacceptability of the method employed.

The cation sum in the Ca site (sum $^{vii} = Ca^{2+} + Sr^{2+} + Ba^{2+}$; $\pm$ 2 sigma = $\pm$ 0.026) varies within the range 0.931–0.992 and thus conveniently never excceds 1.0. Sr^{2+} (max. = 0.017) and Ba^{2+} (max. = 0.007) coexist in this site, but their variation is abrupt and their values are almost low enough to be ignored. However there is a slight tendency for Sr^{2+} to increase when Ca^{2+} decreases, i.e. more Sr in environment III and less in environment II. The difference of the sum from 1.0 is however sufficiently frequent and large to deduce the presence either of some non-analysed cations such as Li^{+}, Y^{3+} or Th^{4+}, or more probably of Mn^{2+} and/or Fe^{2+} presently ascribed to the Ti site in trivalent form, or of Sb^{3+} presently ascribed to the Ti site in pentavalent form. A tendency for the cation sum in the Ca site to be higher in environment II and lower in environment III is detectable.

The cation sum in the Si site (sum $^{iv} = Si^{4+}$ alone; $\pm$ 2 sigma = $\pm$ 0.024) varies in the range 0.967–1.007 with only 3 out of 20 analyses exceeding 1.0 and by such a small amount that one may deduce that, within experimental error, Si overpopulation does not occur. Si deficiency however does occur regularly to a minor extent and could be accommodated by the presence of some $^{iv}Al^{3+}$ or $^{iv}Ti^{4+}$ transferred from the Ti site.

The cation sum in the Ti site (sum $^{vi} = Ti^{4+} + R^{3+} + Sb^{5+}$; $\pm$ 2 sigma = $\pm$ 0.036) always exceeds 1.0 (1.012–1.080) which conveniently provides several cations for satisfying the above-mentioned deficiencies in the Ca and Si sites. A perfect numerical match can of course be obtained since by definition sum $^{(vii + vi + iv)}$ equals exactly 3.0, but there is a considerable choice about which cation to assign to which site. There is always sufficient Al to fill the Si site, but this does not prove the exclusion of the other mentioned possibility: tetrahedral Ti. Generally Cr and Mn are present only as traces and are insufficient alone to explain the deficiences in the Ca site. Although there is not enough Mn to fill the Ca site (as Mn^{2+}) except in 1 case out of 20, there is sufficient $(Mn + Fe)^{2+}$ to fill the Ca site in 19 cases; also there is always enough Sb (as Sb^{3+}) although, as argued below, most Sb is thought to remain in the Ti site in pentavalent form. Our preferred combination is to assign small amounts of Mn^{2+}, Fe^{2+} and/or Sb^{3+} to the Ca site and of Al^{3+} and/or Ti^{4+} to the Si site, in these orders of priority.

In the O(1) anion site linking the octahedra and capable of $O^{2-} = OH^{-}$ and/or $O^{2-} = F^{-}$ heterovalent substitution, the F^{-} values, where analysed, vary abruptly but are always low (max. = 0.024) and they also have a very poor relative standard error due to the rapid loss of F in titanite under the electron beam. The OH^{-} values might well be higher in order to equilibrate the cation charge deficiency caused by the replacement of some Ti^{4+} by R^{3+}. The $OH^{-}_{(calc.)}$ values presented in Tables 3–5 were calculated on the basis of cation/anion charge balance which of course focuses all of the analytical errors into one value which would thus have a low precision and a low accuracy. These initial $OH^{-}_{(calc.)}$ values are always negative in Tables 3 and 5 (because the sum of cation charges always exceeds 10.0 [max. = 10.120], or are < 10.0 but are still too high compared to the analysed F content), but they are mostly reasonable in Table 4. These negative $OH^{-}_{(calc.)}$ values (along with the $O^{2-}_{(calc.)}$ values necessarily exceeding 5 if F = 0.0) constitute the fatal flaw of this particular calculation method for these data. The transfer of any Al^{3+} or Ti^{4+} into the Si site does not of course modify the total charge. Nevertheless one mathematical solution has already been detected above since the transfer of some Mn, Fe and/or Sb from the Ti site to the Ca site involves a reduction in charge. Calculations show that there is always enough Sb, and hence also enough (Mn + Fe + Sb), but not enough (Mn + Fe) without Sb, available for transfer to totally eliminate the excess total cation charge and hence permit the presence of some $OH^{-}_{(calc.)}$, but there is no way of deducing the relative proportions of Mn, Fe and Sb (of which the latter provides twice as much charge reduction). An alternative solution for reducing the overall cation charge is to transform some Sb^{5+} into Sb^{3+} within the Ti site.

It is thus possible to create a perfectly-balanced stoichiometric formula by transfering sufficient Al to fill the Si site, sufficient (Mn + Fe + Sb) to fill the Ca site, transforming all Mn and some Fe from trivalent into divalent and finally transforming sufficient pentavalent Sb into trivalent Sb in order to satisfy overall charge balance and hence eliminate negative $OH^{-}_{(calc.)}$. The only reason why this is not presented in a table is that the mathematical manipulations

involved include too many subjective choices, in particular: whether to preferentially reduce Fe^{3+} or Sb^{5+}, and how much $OH^-_{(calc.)}$ to create, since after eliminating the negative $OH^-_{(calc.)}$ value, one can continue the process to produce some arbitrary positive value.

We may now review the inadequacies of the other possible methods of calculation, on the same initial basis of valencies and co-ordinations.

Fixing sum (vii) = 1.0 (method (*a*)) leads to the unacceptable relation Si > 1.0 in 16 cases out of 20. Worse still, by increasing the number of cations everywhere, and hence increasing the total charge with respect to the values of method (*g*), it produces much greater excesses of $O^{2-}_{(calc.)}$ and very negative $OH^-_{(calc.)}$ values. This confirms the need for extra cations in this site.

Fixing sum (vi) = 1.0 (method (*b*)) reduces all of the cation values and exacerbates the deficiencies in the Ca and the Si sites noted above with method (*g*). If one then proceeded with the transfer of some Mn, Fe, Sb and Al to the other sites as deduced for method (*g*), then method (*b*) will leave the residual octahedral site with notable and undesirable cation vacancies. On the other hand the $OH^-_{(calc.)}$ values would all become positive, and often quite large, due to the total charge and the $O^{2-}_{(calc.)}$ values descending below 10.0 and 5.0 respectively.

Fixing sum (iv) = 1.0 (method (*c*)) leads to sum (vii) just exceeding 1.0 in only 3 cases out of 20. However in 17 cases out of 20 it increases all of the cation values with respect to those of method (*g*) and thus again worsens the situation amongst the anions (e.g. $OH^-_{(calc.)}$ down to −0.364).

Fixing any pair of these single-site sums to equal 2.0 will of course tend to cancel out those aspects with opposite senses and maintain those aspects with the same senses. Since methods (*a*) and (*c*) are equally disastrous for the anions, then there is no point in proceeding with fixing sum (vii + iv) = 2.0 (method (*e*)).

Fixing sum (vi + iv) = 2.0 (method (*f*)), entirely solves the anion problems with reasonable positive values for $OH^-_{(calc.)}$ (0.037–0.206) and both sites vi and iv can have unit occupancy by the simple transfer of Al^{3+} or Ti^{4+} as discussed above, without any changes to the charges. However, the sum (vii) values are all lower than those of method (*g*) and thus create larger cation vacancies in the Ca site without the possibility of transfering any Mn, Fe or Sb from the Ti site since there are no longer any excess cations available there. Thus it is not possible in this situation to conceive of any $^{vii}Mn^{2+}$, $^{vii}Fe^{2+}$ or $^{vii}Sb^{3+}$. However reducing some $^{vi}Sb^{5+}$ to $^{vi}Sb^{3+}$ can increase the $OH^-_{(calc.)}$ value, if desired.

Fixing sum (vii + vi) = 2.0 (method (*d*)) has parallel effects of providing unit occupancy of both sites by simple cation transfer from the Ti site, which, like method (*g*), involves the charge reductions $(Mn,Fe)^{3+}$ to $(Mn,Fe)^{2+}$ and/or Sb^{5+} to Sb^{3+} and hence more $OH^-_{(calc.)}$ production. However with this method there are cation vacancies in the Si site in 17 cases out of 20 which cannot be filled by transforming $^{vi}Al^{3+}$ into $^{iv}Al^{3+}$ without transfering the cation vacancies from one site to the other.

It can be seen then that methods (*d*) and (*f*) of summing two sites to 2.0 cations, especially method (f), represent improvements with respect to the more extreme methods (*a*), (*b*) and (*c*) of summing single sites to 1.0 cation; they nevertheless still have serious problems which are analogous (cation vacancies) but concern different sites, and they are not obviously better than the initial method (*g*).

This evaluation leads to the conclusion that the real situation in the structural formulae of these titanites lies somewhere between the values calculated by methods (*g*) and (*f*), but closer to method (*g*), followed by at least partial transfer of the indicated cations to exactly fill the tetrahedral and octahedral sites and to eliminate negative $OH^-_{(calc.)}$.

If the initial basis is modified, e.g. by fixing all Fe as $^{vii}Fe^{2+}$ rather than $^{vi}Fe^{3+}$, then a new evaluation of methods (*a*) to (*g*) will yield different intermediate results, but the final result after certain necessary valency and/or co-ordination adjustments, will probably be very similar with the same doubts over Fe^{3+} *vs.* Sb^{5+} reduction, and over how much $OH^-_{(calc.)}$ to create.

Crystal-chemistry: 3

Correlations between cation variations

The values plotted in Figs. 6–9 correspond to Tables 3–5 and do not take into account the various possibilities of changing valencies and/or co-ordinations and/or structural formula method (as discussed above) which may or may not cause the values to change; thus in each case the total element content on the basis of structural formula method (g) is being plotted. The following observations are made:

(i) Fig. 6*a,b,c* presents, for the environments I, II and III respectively, cation plots of Sb^{5+}, Al^{3+}, Cr^{3+} and Fe^{3+} against Ti^{4+}; Mn^{3+} is excluded because of its low values and the fact that they remain fairly constant across each table. There is clearly a moderately-good negative correlation between Sb and Ti in each environment (correlation coefficient r = 0.92–0.96), but the ranges of the absolute values are different. There also exists, of course, the inherent mathematical constraint of the constant sum of $^{vi}(R^{2+} + R^{3+} + R^{4+} + R^{5+})$ which, if really constant in the data-set, would partially impose a

negative correlation of Ti with any one of the other cations, in particular the most abundant one: Sb.

(ii) There are also negative correlations between Al^{3+} or Fe^{3+} with Ti^{4+} in environments II and III (r = 0.86–0.97), again with different ranges of the absolute values, but not in environment I. Hence in environments II and III there are positive correlations between Al^{3+}, Fe^{3+} and Sb^{3+}.

(iii) Cr^{3+} is absent from environment II, insignificantly present in environment III, but significantly present in environment I where it sometimes exceeds the values of Al^{3+} and Fe^{3+}. Given that Cr^{3+} often follows Fe^{3+} or Al^{3+} in several kinds of silicate mineral (e.g. garnet, pyroxene...), it is deduced that in environment I Cr^{3+} has partially replaced Al^{3+} and Fe^{3+} (and also Mn^{3+} in Table 3) and thus deranged the supposed negative trends with Ti^{4+}. This is supported by the flagrant antipathetic behaviour of the Al^{3+} and Fe^{3+} values on the one hand and the Cr^{3+} values on the other in Fig. 6a.

(iv) Fig. 7 plots the sum $R^{3+} = [Al^{3+} + Cr^{3+} + Mn^{3+} + Fe^{3+}]$ (N.B. without any Sb^{3+} allowed) against Ti^{4+} for each environment (r = 0.87–0.96). Compared to Fig. 6 the correlations improve slightly for Cr-poor environments II and III and a real correlation appears for environment I; this thus confirms that Cr^{3+} contributes to the total R^{3+} by replacing one of the other trivalent cations rather than by adding to the total. Henceforth only R^{3+} is used for plotting.

(v) Fig. 8 plots Sb^{5+} against R^{3+} for each environment. This displays moderately-good positive correlations (r = 0.86–0.98) but again with different ranges of absolute values.

(vi) From the raw data presented above it may be concluded that the same kind of trend occurs within each petrographical environment, but that different ranges of absolute values are involved. The data from the three environments may thus be combined in order to observe the overall correlations and especially the slopes of the least-squares 'best line'. The combined data set of Fig. 9 shows good correlations for each pair of the three key variables Ti^{4+}, R^{3+} and Sb^{5+} (r = 0.93–0.96) with only two samples noticeably distinct.

(vii) The slope of Sb^{5+} *vs.* Ti^{4+} (−0.61) is closer to that required by equation (23) (0.50) than to that required by equation (21) (with all Sb^{3+} plotted as Sb^{5+}) (1.00). This could mean that both of these substitutions operate simultaneously with more of (23). Alternatively it could mean that substitution (23) operates alone and that the apparent excess of Sb is actually trivalent in the Ca site ($^{vii}Sb^{3+}$). It cannot be explained by substitution (21) alone because of a great deficit of total Sb. Note that the best line passes through the origin at Sb = 0.00, Ti = 1.00, within the limits of ± 2 sigma for Ti.

(viii) The slope of R^{3+} *vs.* Ti^{4+} (- 0.43) is somewhat lower than that required by substitution (23) (0.50) and is much further from that required by equation (18) (1.00) combined with a charge-balancing equation such as (13), or (4) (which necessitates adjusting the valency of Sb). There is thus insufficient R^{3+} compared to Sb^{5+} for equation (23). This supports the above suggestion that equation (21) is also operative since the required transformation of some Sb^{5+} into Sb^{3+} reduces the real value of Sb^{5+} (and increases the effective R^{3+} by adding some Sb^{3+}). However the best line misses the origin at Ti = 1.00, and does so with an excess rather than a deficit of R^{3+}. This indicates the need to displace significant amounts of R^{3+}, such as Al^{3+} to the Si site and Mn^{3+} and/or Fe^{3+} to the Ca site in divalent form, as indicated above on the basis of cation sums, and argues against placing any Ti^{4+} in the Si site.

(ix) The slope of Sb^{5+} *vs.* R^{3+} (+ 1.29) exceeds that required by substitution (23) (1.00) since it reflects the excess of the former and the deficit of the latter, with respect to Ti^{4+}, as observed above. Likewise the best line again misses the origin at Sb = 0.00 with a similar excess of R^{3+} (around 0.05 cations).

(x) Algebraically combining 80% of substitution (23) with 20% of substitution (21) gives the following slopes for the three plots of Fig. 9: −0.60, −0.40 and +1.5. These compare favourably with the slopes of the data of Fig. 9 and thus support the predominance of this combination of substitutions as suggested above. However since there exists no unique solution in terms of coupled substitutions, nor in terms of the method of structural formula calculation, nor in terms of the attributions of cation valencies and co-ordinations, no further precisions or deductions are attempted. It is nevertheless considered that, within the limits of the analytical uncertainty (Tables 3–5), the data treatment presented above has allowed the deduction of several confident conclusions along with reasonably-good indications of several other features, as summarized below.

Conclusions

(1) Sb is usually the most abundant cation (up to 0.165 Sb per Si = 1.000) other than Ca, Ti and Si in Sb-rich titanites from three different syn- or post-greenschist petrographical environments in the manganese concentrations at St. Marcel-Praborna, Aosta Valley, Italy.

(2) Each of these different petrographical environments (I. 'the emerald-green horizon'; II. 'late-stage cm-sized veinlets'; III. 'microfissured late-stage mm-sized veinlets') display different crystal-chemical, and hence geochemical, features.

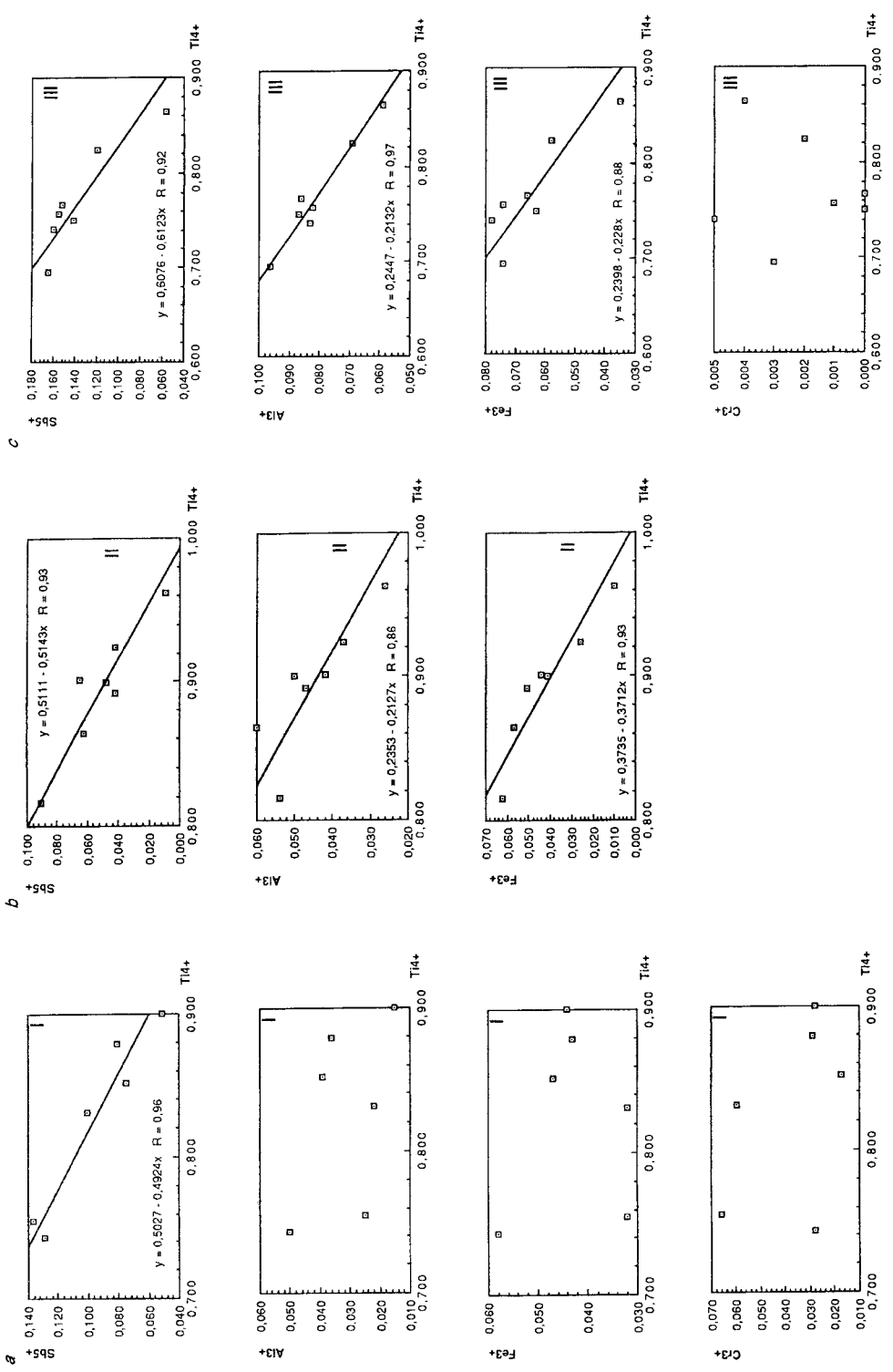

FIG. 6. Plots of Sb^{5+}, Al^{3+}, Fe^{3+} and Cr^{3+} against Ti^{4+} for environments I (*a*), II (*b*) and III (*c*). Note that the cation scales, normalized for maximum visibility, are variable (also for Figs. 7–8).

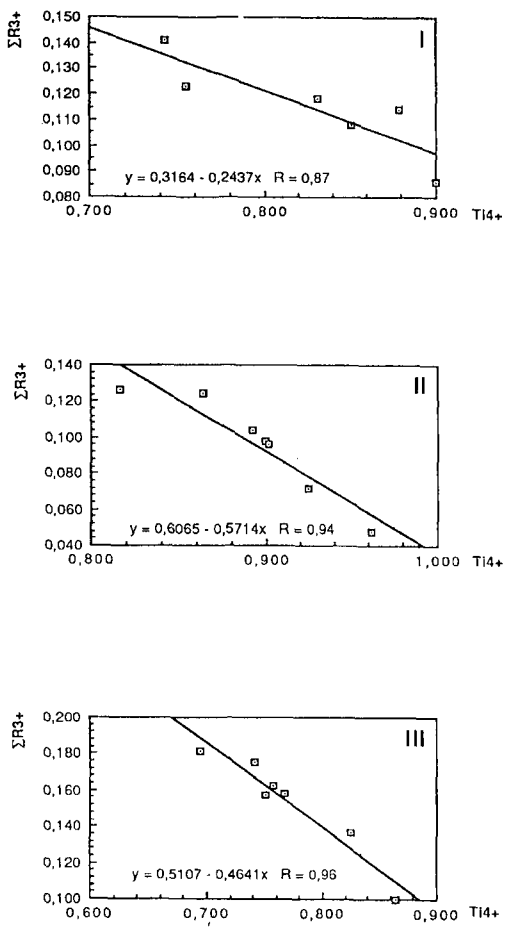

FIG. 7. Plots of sum R^{3+} against Ti^{4+} for environments I, II and III.

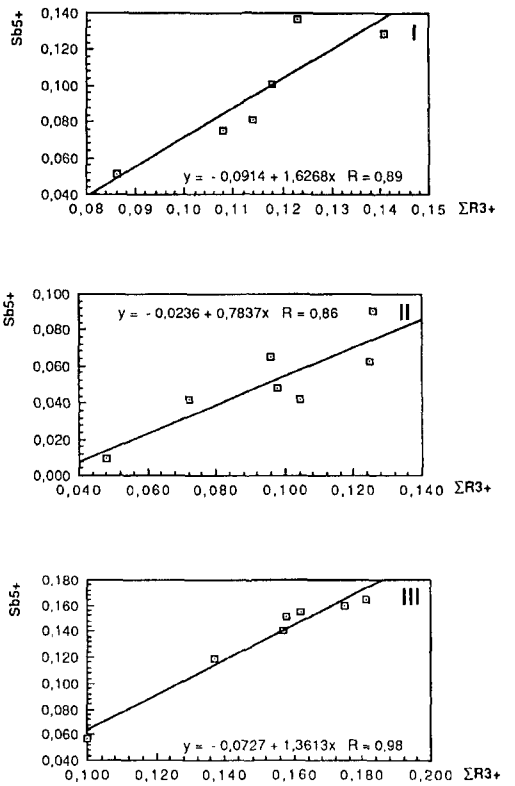

FIG. 8. Plots of Sb^{5+} against sum R^{3+} for environments I, II and III.

(3) The Sb contents are zoned and are highest alongside grain boundaries, microfractures, pores and inclusions.

(4) The presence of Sb is generally accompanied by Al, Cr, Mn, Fe, Sr, Ba and F and most probably also OH; all these elements having been mobilized at a very late stage in the evolution of the manganese concentrations; Ti is now added to the list of late-mobilized elements.

(5) The Mn contents of the titanites are generally lower than those in the published analyses of the pink variety of titanite called 'greenovite'.

(6) Detailed evaluations of several different options for calculating the structural formula and for attributing valencies and co-ordinations to each element, and hence for establishing ion substitutions and their combinations, lead to the conclusions that:

— method (*g*) for the structural formula is superior to all the others on condition that the negative $(OH)^-_{(calc.)}$ values are eliminated by total charge reduction by reducing some Mn^{3+} and/or Fe^{3+} to divalent form and some Sb^{5+} to trivalent form; the formula may be improved by algebraically incorporating a small proportion of method (*f*) to allow minor cation vacancies in the Ca site; there are no objective criteria available for specifying the extent of these data manipulations except for the necessity of overall charge balance, but there is no unique solution for this; the two main problems concern how much $OH^-_{(calc.)}$ to create by reduction of Fe^{3+} and/or Sb^{5+}, and which of these cations to reduce in preference;

— the Ca site is occupied by Ca^{2+}, Sr^{2+}, Ba^{2+}, Mn^{2+}, Fe^{2+} and possibly also Sb^{3+}, in this order of priority;

— the Ti site is occupied by Ti^{4+}, Sb^{5+}, Cr^{3+}, Al^{3+}, Sb^{3+}, Fe^{3+} and possibly also Mn^{3+}, in this order of priority;

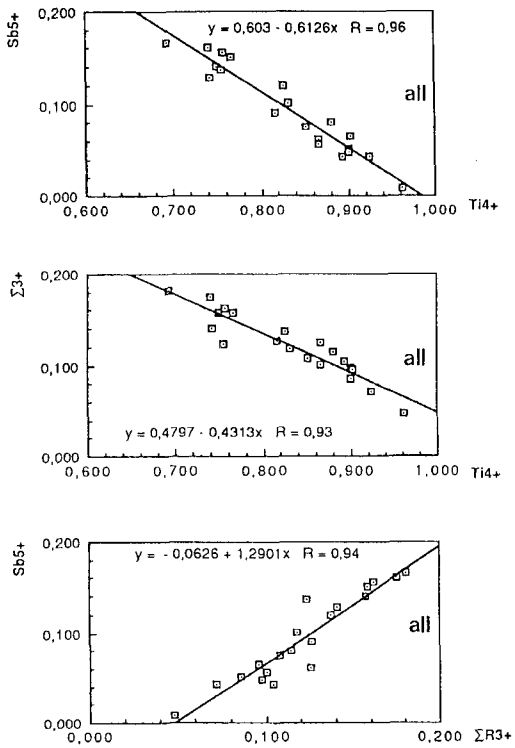

FIG. 9. Plots of Sb^{5+}, Ti^{4+} and sum R^{3+} against each other with the combined data from all three environments (n = 20).

— the Si site is occupied by Si^{4+} and Al^{3+}, in this order of priority;
— the O1 site is occupied by F^-, OH^- and O^{2-}, in this order of priority;
— most Sb is pentavalent; trivalent Sb is more necessary in the Ti site than in the Ca site; hence both valencies 3+ and 5+ must occur for Sb in this natural silicate and apparently both occur in the same site.
— the overall cation substitutions compared to pure ideal titanite may be adequately described by a combination of equations (2), (4), (8), (13), (21) and (23) in which (23) predominates by far; equation (26) might however be more realistic than (21).

(7) Four hypotheses can largely explain the fate of the Ti expelled by the Sb-metasomatism of pre-existing titanites:

(i) incorporation into newly-formed Sb-rich rutile microinclusions;

(ii) incorporation into newly-formed overgrowths of Sb-rich titanite;

(iii) incorporation into newly-formed very late fuzzy Ti-bearing braunite; or

(iv) incorporation into Ti-bearing hollandites. Evidence exists to support each hypothesis; (i) is more appropriate to environment III, whereas (iii) and (iv) are more appropriate to environment II.

(8) Finally the data establish that metasomatism by Sb was a very late petrological event at St. Marcel (later than the Sr- and Ba-metasomatisms which at an earlier stage created the Sr- and/or Ba-bearing hollandite, piemontite, apatite and carbonates), and that this Sb entered in significant amounts only into the titanite, rutile and roméite structures.

Acknowledgements

We are grateful to G. Hamm (Muséum National d'Histoire Naturelle, Paris) for carefully preparing the thin sections and to P. Blanc (Université Paris VI) for efficiently helping with the SEM technique. G. Ilinca (University of Bucharest) and A. Mottana (University of Rome) kindly contributed to ameliorations of the text.

References

Bernau, R. and Franz, G. (1987) Crystal-chemistry and genesis of Nb-, V-, and Al-rich metamorphic titanite from Egypt and Greece. *Canad. Mineral.*, **25**, 695–705.

Černý, P. and Povondra, P. (1972) An Al,F-rich metamict titanite from Czechoslovakia. *Neues Jahrb. Mineral., Mh.*, 400–6.

Clark, A.M. (1974) A tantalum-rich variety of sphene. *Mineral. Mag.* **39**, 605–7.

Colomba, L. (1910) Rhodonite cristallizzata di St. Marcel (Valle d'Aosta). *Atti R. Acc. Sc. Torino*, **39**, 664–68.

Deer, W.A., Howie, R.A. and Zussman, J. (1982) Orthosilicates. *Rock-forming Minerals, 1A*, Longman, London, 919 pp.

Dufrenoy, A. (1847) *Traité de minéralogie*. Paris, 3, 669–71.

Fermor, L.L. (1908) The manganese deposits of India. *Mem. Geol. Survey India*, **37**, 1–1158.

Gibert, F., Moine, B. and Gibert, P. (1990) Titanites (sphènes) alumineuses formées à basse/moyenne pression dans les gneiss à silicates calciques de la Montagne Noire. *Comptes Rendus Acad. Sci., Paris, Série II*, **311**, 657–63.

Groat, L.A., Carter, R.T., Hawthorne, F.C. and Ercit, T.S. (1985) Tantalian niobian titanite from the Irgon Claim, Southeastern Manitoba. *Canad. Mineral.*, **23**, 569–71.

Heslop, R.B. and Robinson, P.L. (1963) *Inorganic Chemistry: a guide to advanced study*. Elsevier, Amsterdam, 591 pp.

Kienast, J.-R., Smith, D.C. and Martin, S. (1982) Jadeite-acmite solution and the behaviour of manganese in the HP-LT pyroxenes at Praborna, Val d'Aosta, Italy. *Terra Cognita*, **2(3)**, 332–3.

Lom de, B. (1843) La découverte de la greenovite et de la roméine. *Feuilles d'annonces d'Aoste*, 3.

Martin, S. and Kienast, J.-R. (1987) The HP-LT manganiferous quartzites of Praborna, Piemont ophiolite nappe, Italian Western Alps. *Schweiz. Mineral. Petrogr. Mitt.*, **67**, 339–60.

Martin-Vernizzi, S. (1982) La mine de Praborna (Val d'Aoste, Italie): une série manganésifère métamorphisée dans le faciès éclogite. *Thèse 3ème cycle, Univ. Paris VI*, 215 pp.

Maury, R., Perseil, E.A., Berbeleac, I. and Tanasescu, I. (1993) L'alabandite (MnS), ses associations, ses paragenèses complexes: cas des Hautes Pyrénées (France) et des Monts Métallifères (Transylvanie-Roumanie). *Romanian J. Mineral.*, **76**, 63–9.

Millosevich, F. (1906) Sopra alcuni minerali di Val d'Aosta. *Rend. R. Acc. Lincei, Roma*, **15**, 317–21.

Mottana, A. (1986) Blueschist-facies metamorphism of manganiferous cherts: A review of the alpine occurrences. *Geol. Soc. Amer. Memoir*, **164**, 267–99.

Mottana, A. and Griffin, W.L. (1979) Pink titanite (greenovite) from St. Marcel, Valle d'Aosta, Italy. *Rend. Soc. Ital. Mineral. Petrol.*, **35**, 135–43.

Mottana, A., Rossi, G., Kracher, A. and Kurat, G. (1979) Violan revisited: Mn-bearing omphacite and diopside. *Tschermaks Min. Petr. Mitt.*, **26**, 187–201.

Oberti, R., Smith, D.C., Rossi, G. and Caucia, F. (1991) The crystal-chemistry of high-aluminium titanites. *Euro. J. Mineral.*, **3**, 777–92.

Pascal, P. (1958) *Nouveau Traité de Chimie Minérale*: Tome XI: arsenic - antimoine - bismuth. Masson, Paris.

Paul, B.J., Černý, P. and Chapman, R. (1981) Niobian titanite from the Huron Claim pegmatite, Southeastern Manitoba. *Canad. Mineral.*, **19**, 549–52.

Perseil, E.-A. (1985) Quelques caractéristiques des faciès à oxydes de manganèse dans le gisement de St. Marcel-Praborna (Val d'Aoste, Italie). *Mineral. Deposita*, **20**, 271–6.

Perseil, E.-A. (1987) Particularités des piémontites de Saint-Marcel-Praborna (Italie): Spectres I.R. *Actes du 112e Congrès National Sociétés Savantes, Lyon*, Section Sciences, Fascicule I, 209–15.

Perseil, E.-A. (1988) La présence du strontium dans les oxydes manganésifères du gisement de St. Marcel-Praborna (Val d'Aoste, Italie). *Mineral. Deposita*, **23**, 306–8.

Perseil, E.-A. (1991) La présence de Sb-rutile dans les concentrations manganésifères de St. Marcel-Praborna (Val d'Aoste, Italie). *Schweiz. Mineral. Petrog. Mitt.*, **71**, 341–7.

Post, J.E. and Bish, D.L. (1989) Rietveld refinement of the coronadite structure. *Amer. Mineral.*, **74**, 913–7.

Ribbe, P.H. (1980) Titanite (sphene). Ch. 6 in *Orthosilicates*, (P.H. Ribbe, ed.), Reviews in Mineralogy, **5**, 137–54.

Rota, J.C. and Hausen, D.M. (1991) Geology of the Gold Quarry mine. *Ore Geol. Rev.*, **6**, 83–105.

Russell, J.K., Groat, L.A. and Halleran, A.A.D. (1994) LREE-rich niobian titanite from Mount Bisson, British Columbia: chemistry and exchange mechanisms. *Canad. Mineral.*, **32**, 575–87.

Sahama, Th.G. (1946) On the chemistry of the mineral titanite. *C. R. Soc. Geol. Finlande*, **19** (138), 88–120.

Shannon, R.D. (1976) Revised effective ionic radii and systematic studies of interatomic distances in halides and chalcogenides. *Acta Cryst.*, **A32**, 751–67.

Smith, D.C. (1981) The pressure and temperature dependence of Al-solubility in sphene in the system Ti-Al-Ca-Si-O-F. *Progress Experiment. Petrol. NERC Pub. London*, Series **D18**, 193–7.

Smith, D.C. (1988) A review of the peculiar mineralogy of the 'Norwegian Coesite-Eclogite Province', with crystal-chemical, petrological, geochemical and geodynamical notes and an extensive bibliography. Pp. 1–206 in *Eclogites and Eclogite-Facies Rocks*, (D.C. Smith, ed.), Developments in Petrology, **12**, Elsevier, Amsterdam, 524 pp.

Smith, D.C. and Perseil, E.-A. (in prep.) Pentavalent antimony in Sb-rich rutile from St. Marcel-Praborana, Aosta Valley, Italy.

Zachariasen, W.H. (1930) The crystal structure of titanite. *Zeit. Krist.*, **73**, 7-16.

[*Manuscript received 1 August 1994: revised 25 January 1995*]